SSRG International Journal of Electrical and Electronics Engineering
ISSN: 2348-8379/ https://doi.org/10.14445/23488379/IJEEE-V10I5P104

Volume 10 Issue 5, 36-47, May 2023

Original Article

A New Optimizing Approach to Minimize Power Losses of an Electric Power Grid Containing Major Loads of Huge Power 3-Phase Induction Machines – A Practical Case Study in Vietnam

Tien-Dung Nguyen[1], Ngoc-Quang Dinh[2], Ngoc-Khoat Nguyen[1*], Thi-Duyen Bui[1], Anh-Tuan Bui[3], Trung-Dung Pham[4]

[1]*Faculty of Control and Automation, Electric Power University, Hanoi, Vietnam*
[2]*Innovative Grid Solutions Vietnam JSC, Hanoi, Vietnam*
[3]*Hanoi Textile and Garment Industry University, Hanoi, Vietnam*
[4]*Le Quy Don Technical University, Hanoi, Vietnam*

[1*]*Corresponding Author : khoatnn@epu.edu.vn*

Received: 03 March 2023 Revised: 11 April 2023 Accepted: 04 May 2023 Published: 29 May 2023

Abstract - *Induction machines play an important role in popular electrical loads, leading to many relevant control methods. One of the most crucial control strategies is to design an efficient method to minimize power losses against continuous and random voltage variation. This paper proposes a novel optimal scheme to minimize power losses of loads containing 3-phase induction motors, considered critical loads of an electric power grid. The study evaluates the effects of the voltage fluctuation on the 3-phase induction AC motors, presenting an effective method to design a newly reactive power compensator. This compensated system includes decentralized compensators at each load together with a central compensator unit using only one common controller to optimize the operation and efficiency of the whole network. The paper introduces a step-by-step procedure to control reactive power compensation capacity for each induction motor, improving voltage quality at loads, reducing active power losses, and prolonging the devices' lifespan. Simulation results and experiments are also provided to demonstrate the effectiveness and applicability of the proposed method.*

Keywords - *3 Phase induction motors, Voltage variation, Reactive power compensator, Motor efficiency.*

1. Introduction

High power quality in a grid is extremely important, allowing electric equipment to operate under optimal conditions. In this context, power losses are minimized, the lifetime of devices is prolonged, and the efficiency of equipment is improved, leading to economical operation and distribution of the electric power network. This also ensures a meaningful decrease in overall energy consumption and thus protects devices and customers' health [1-10]. It is clear that poor power quality strongly affects the operation of electrical equipment, especially induction motors, which are the most common loads in power distribution systems (accounting for 45 – 50% capacity of all loads) [11-18]. These AC machines highly suffer from poor power quality, concentrating on the following issues:

(1) According to NEMA curves shown in Figure 1 [19-20], voltage deviations strongly cause the induction motor's efficiency to be significantly decreased. As presented in Figure 1, consider the EFF curve. If the voltage is reduced by 5% from the rated one, the induction motor efficiency is down by about 1%. Meanwhile, a 10% - voltage variation will cause the efficiency to decrease by about 3-4%.

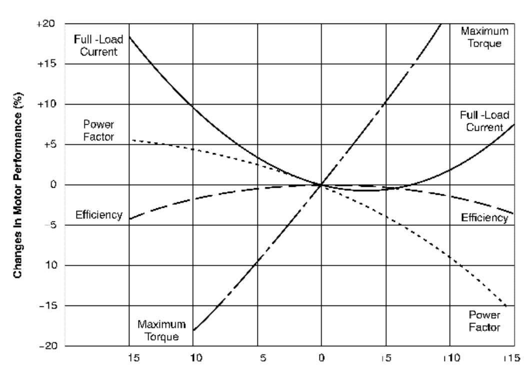

Fig. 1 Changes in induction motor efficiency regarding voltage variations [19-20]

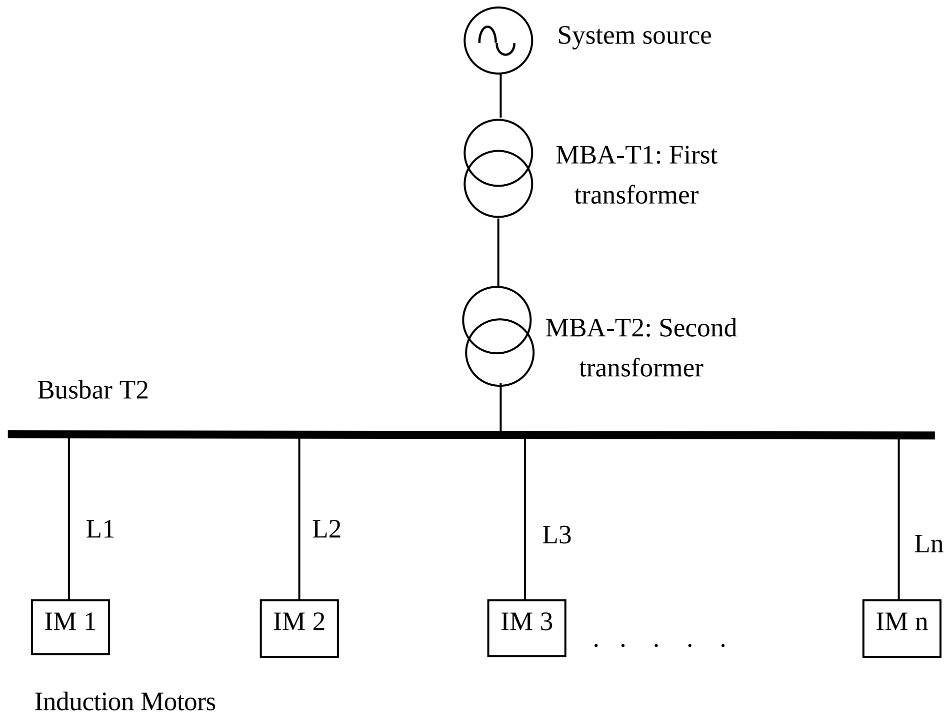

Fig. 2 The schematic diagram of an electric power grid

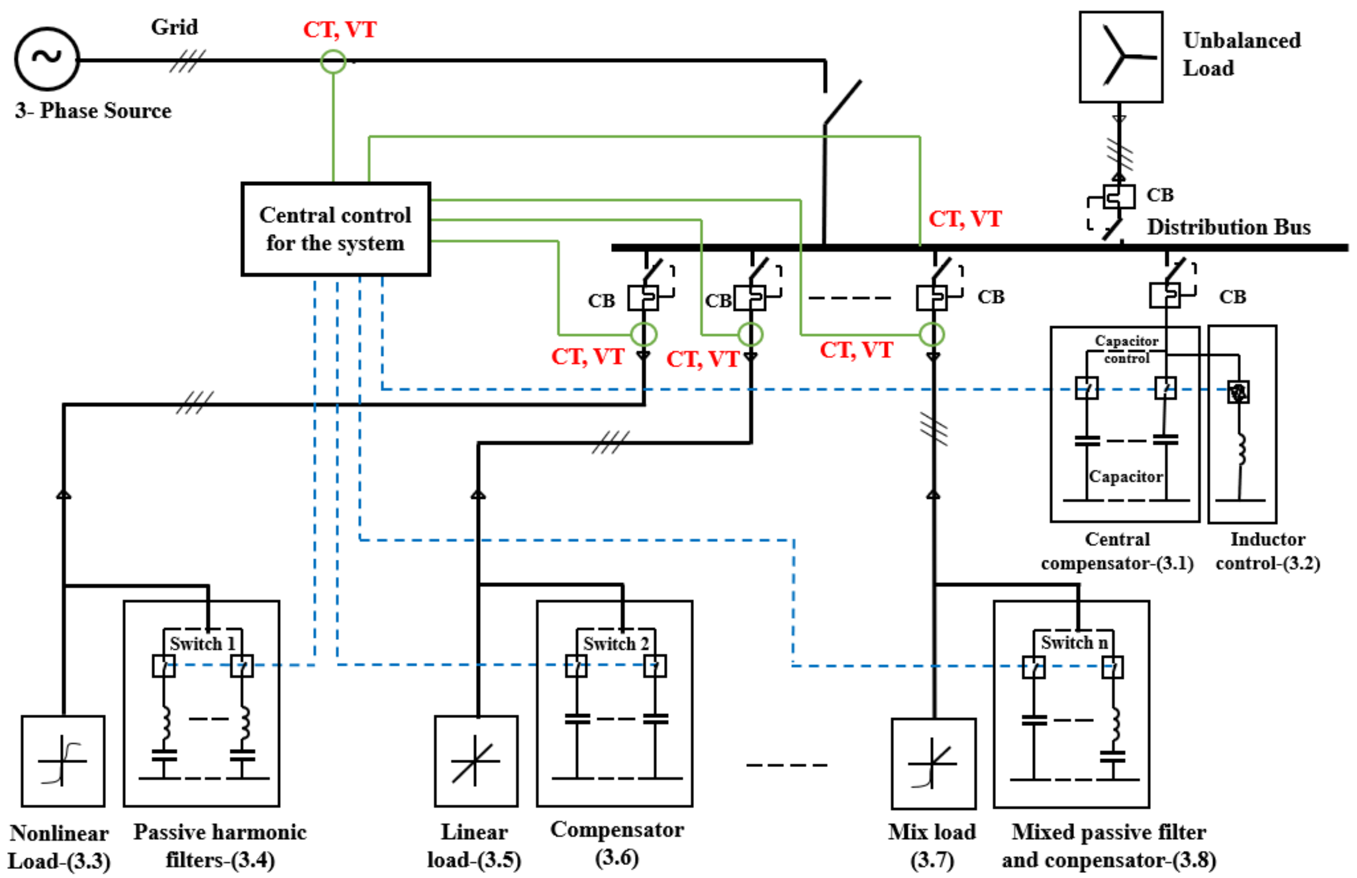

Fig. 3 Principle diagram of a system containing several decentralized compensators and one centralized controller

(2) Low power factors, cosφ units, cause huge losses on the cables and transformers. These low factors also affect the voltages at induction motors, leading to a dramatic decrease in efficiency and an unwanted increase in loss [10-12].
(3) The three-phase unbalanced voltage also affects the efficiency of the induction motor [11-12]. If the deviation is large, it will cause the induction motor to be vibrated and shake, increasing losses. Therefore, it is necessary to keep this index below 2%.
(4) Harmonic distortion also affects the efficiency of asynchronous induction motors [12], [21-26]. Depending on the spectrum of harmonics and waveforms, additional losses in the induction motors can be caused by distorting the electromagnetic field pattern. This phenomenon also causes skin effects leading to heating-up electric motors. Some types of harmonics, such as rectangular waves, can cause electric motor losses to increase by up to 30-35%.

These effects can be overcome by adding voltage regulation devices, reactive power compensators and harmonic filters, which significantly increase system efficiency, reduce losses and prolong equipment lifetime. The goal of this study mainly focuses on determining the optimal method to compensate reactive power to minimize losses for the induction motors. Considering a typical electric power grid illustrated in Figure 2, the mainly centralized compensators are mounted on the busbar of the transformer MBA-T2. Under these conditions, active power loss on L1, L2, and Ln transmission lines cannot be decreased. Furthermore, the voltage drops on these lines are pretty large, causing the efficiency of asynchronous induction motors (IM i; i = 1 ÷ n) to decrease as shown in Figure 2. Therefore, the current paper proposes a voltage regulator consisting of distributed reactive power compensators and a centralized controller.

The rest of this paper is as follows. In Section 2, the design of a decentralized voltage regulation in combination with a centralized controller will be introduced in detail. Next, Section 3 presents simulation and practical results for the proposed compensation scheme. Finally, conclusions and future work raised from this study will be provided in Section 4.

2. Decentralized Voltage Regulation Using A Centralized Controller

Significant power influences quality on the performance of asynchronous AC motors, including considerable voltage deviations, low power factor, unbalance voltage and harmonics, should be known. In this study, a new scheme applying decentralized reactive power compensators together with a centralized controller is proposed. The schematic diagram is depicted in Figure 3.

2.1. Major Components of the System

2.1.1. Central Control for the System

The control centre consists of many measurement systems calculating power at each branch through current and voltage signals. Here, the reactive power compensation and voltage regulation process can be calculated by combining power changes in the peripheral and central devices. Centre reactor device (3.2): The purpose of smoothening power regulation is to smoothen the voltage of the network.

2.1.2. Central Reactive Power Compensation Device (3.1)

The objective of this component is to compensate the necessary reactive power for the voltage regulation system or replace a faulty peripheral device. Peripheral devices (3.4), (3.6) and (3.8) are capacitor-type devices or stepwise switching harmonic filter branches located at distributed load systems (3.3), (3.5) and (3.7). Here, the harmonic filter (3.4) is used to compensate for reactive power and to filter the harmonics of nonlinear loads. Meanwhile, the reactive power compensator (3.6) compensates reactive power for linear loads. Finally, the reactive power compensator (3.8) is employed for both functions: harmonics filtering and reactive power compensating for mixed loads (3.7), including linear and nonlinear ones.

2.2. Working Principle

The central controller executes the calculation of power compensation for each branch of loads. Then, the power regulation of the peripheral device is combined with the adjustment of the firing angle of the central reactor. It is noted that closing a branch of a distributed device should be combined with a position change of the reactor firing angle α to position α_{min}. The next step is to adjust the firing angle until the desired optimum power is achieved. Power adjustment at peripheral devices can be implemented according to power factor, voltage, or reactive power.

The application of distributed voltage regulators integrated with centralized compensators assists with optimising power losses on the transmission lines, in the compensator and at the electric motors. To the specific understanding, an equivalent circuit corresponding to the typical power network shown in Figure 2 is used, as illustrated in Figure 4. With the compensating devices placed at the end of the cables, it is significant to calculate the system's parameters following the secondary side of the transformer MBA-T2. Here, the power loss of the synchronous induction motor caused when using the compensators is as follows [22]:

$$\Delta P = R_{td}\frac{P_{tt}^2+(Q_{tt}-Q_b)^2}{U_{ht}{}^2}.10^{-3}+\Delta p_b.Q_b+P_{tt}.\left[1-\eta_{\max}-\Delta\eta\left\{Q_{tt}-Q_b\right\}\right] \quad (1)$$

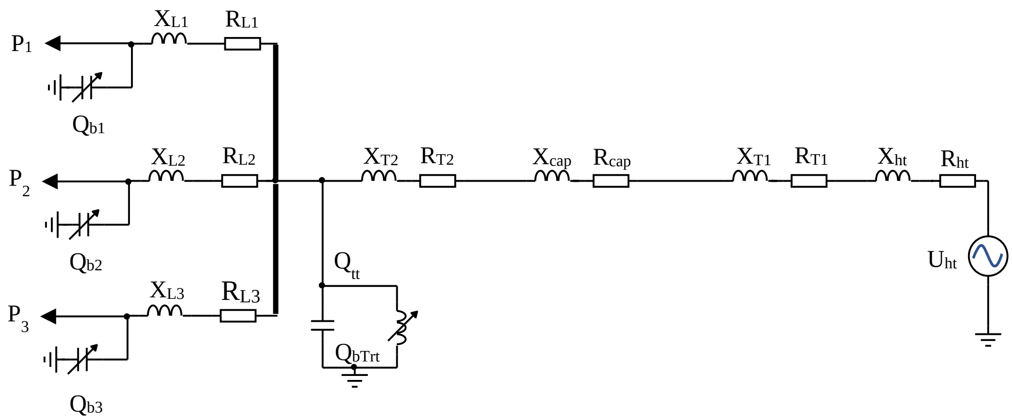

Fig. 4 An equivalent grid diagram for induction motors, including compensators

Where,

R_{td} - equivalent resistor of the system; P_{tt}, Q_{tt}: active and reactive of the loads; Δp_b- loss of active power of the compensator; Q_b- reactive compensation; η_{max}- maximum efficiency of the load; $\eta\{Q_{tt}-Q_b\}$- change of efficiency in percentage.

The power loss can be classified into three components: line resistors, losses of compensators and induction motors' losses.

To determine the optimal power compensation, it is necessary to compute Q_{bi} if the first–order derivative of ΔP reaches zero.

$$\frac{\partial \Delta P}{\partial Q_b} = -2R_{td}\frac{(Q_{tt}-Q_b)}{{U_{ht}}^2}.10^{-3} + \Delta p_b - P_{tt}.\frac{\partial \Delta\eta\{Q_{tt}-Q_b\}}{\partial Q_b} = 0 \quad (2)$$

Remember that efficiency changes of the electric machines belong to voltage variations as plotted in the NEMA curve (see Figure 1). These curves can be approximately described as the following relationship:

$$\Delta\eta\{Q_{tt}-Q_b\} = (K_1.\Delta U_{Dc}^2 + K_2.\Delta U_{Dc} + C).10^{-2} \quad (3)$$

Where K_1, K_2 and C denote constant factors which are determined from the experiment curves, i.e. NEMA – EFF shown in Figure 1. It is noted that these factors are determined precisely for each type of induction machine.

Where ΔU_{Dc} is calculated in percentage form as:

$$\Delta U_{Dc} = \frac{U_{Dc}-U_{dm}}{U_{dm}}.100 = \frac{U_{ht1}.10^3-U_{dm}-\Delta U}{U_{dm}}.100 \quad (4)$$

$$U_{ht1} = \frac{U_{22}}{U_{11}}U_{ht} \quad (5)$$

$$\Delta U = \frac{P_{tt}.R_{td}+(Q_{tt}-Q_b)X_{td}}{U_{ht}} \quad (6)$$

Where ΔU denotes voltage drop in transmission lines and transformers.

From Equation (2), it is straightforward to deduce the following:

$$\frac{\partial\Delta\eta\{Q_{tt}-Q_b\}}{\partial Q_b} = \left(2K_1.\Delta U_{Dc}.\frac{\partial\Delta U_{Dc}}{\partial Q_b} + K_2.\frac{\partial\Delta U_{Dc}}{\partial Q_b}\right) \times 10^{-2} \quad (7)$$

Determining similar values above, the optimal reactive power compensation at each load is computed as follows:

$$\begin{cases} Q_b = Q_{tt} + \frac{A_3 - A_2.\Delta p_{b1}}{A_1} \\ A_1 = 2R_{td}.10^{-3}.U_{dm}^2 - 2.10^2.K_1.P_{tt}.{X_{td}}^2; \\ A_2 = (U_{dm}.U_{ht})^2 \\ A_3 = P_{tt}.X_{td}.\{2.10^2K_1[(U_{ht1}.10^3 - U_{dm})U_{ht} - P_{tt}.R_{td}] + K_2U_{dm}U_{ht}\} \end{cases} \quad (8)$$

For a case study, let us consider a factory containing three induction motors located at different positions. A schematic diagram to deal with the calculation of optimal power compensations is depicted in Figure 5.

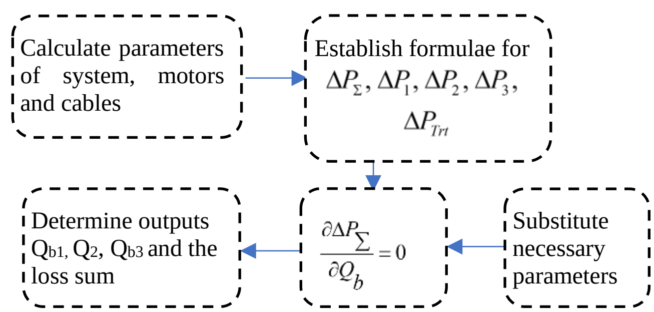

Fig. 5 A step-by-step block diagram to determine reactive power compensations

The total power losses are calculated as follows:

$$\Delta P_\Sigma = \Delta P_1 + \Delta P_2 + \Delta P_3 + \Delta P_{Trt} \quad (9)$$

Where ΔP_1, ΔP_2, ΔP_3 denote losses of three induction motors to the system and they are computed as follows:

$$\Delta P_1 = R_1 \frac{P_1^2 + (Q_1 - Q_{b1})^2}{U_{TC}^2}.10^{-3} + \Delta p_{b1}.Q_{b1} + P_1.\left[1 - \eta_{1\max} - \Delta\eta_1\left\{Q_1 - Q_{b1}\right\}\right] \quad (10)$$

$$\Delta P_2 = R_2 \frac{P_2^2 + (Q_2 - Q_{b2})^2}{U_{TC}^2}.10^{-3} + \Delta p_{b2}.Q_{b2} + P_2.\left[1 - \eta_{2\max} - \Delta\eta_2\left\{Q_2 - Q_{b2}\right\}\right] \quad (11)$$

$$\Delta P_3 = R_3 \frac{P_3^2 + (Q_3 - Q_{b3})^2}{U_{TC}^2}.10^{-3} + \Delta p_{b3}.Q_{b3} + P_3.\left[1 - \eta_{3\max} - \Delta\eta_3\left\{Q_3 - Q_{b3}\right\}\right] \quad (12)$$

It is noted that the central loss compensation ΔP_{Trt} is considered below:

$$\Delta P_{Trt} = R_{td} \frac{P_\Sigma^2 + (Q_\Sigma - Q_{b\Sigma} - Q_{bTrt})^2}{U_{ht1}^2}.10^{-3} + \Delta p_{bTrt}.Q_{bTrt} \quad (13)$$

Where
$$\begin{cases} P_\Sigma = P_1 + P_2 + \cdots + P_3 \\ Q_\Sigma = Q_1 + Q_2 + Q_3 \\ Q_{b\Sigma} = Q_{b1} + Q_{b2} + Q_{b3} \end{cases} \quad (14)$$

To determine the optimal compensation for the three-induction motor system, it is necessary to calculate the first–order derivative of Q_b as follows:

$$\frac{\partial \Delta P_\Sigma}{\partial Q_b} = \begin{bmatrix} \frac{\partial \Delta P_\Sigma}{\partial Q_{b1}} \\ \frac{\partial \Delta P_\Sigma}{\partial Q_{b2}} \\ \frac{\partial \Delta P_\Sigma}{\partial Q_{b3}} \\ \frac{\partial \Delta P_\Sigma}{\partial Q_{bTrt}} \end{bmatrix} = 0 \quad (15)$$

Substituting Equations (10)-(13) to Equation (9) and in combination with Equation (15), one can be obtained below:

$$\begin{cases} \frac{\partial \Delta P_1}{\partial Q_{b1}} = -2R_1 \frac{(Q_1 - Q_{b1})}{{U_{TC}}^2}.10^{-3} + \Delta p_{b1} - P_1.\frac{\partial \Delta\eta_1\{Q_1 - Q_{b1}\}}{\partial Q_{b1}} \\ \frac{\partial \Delta P_2}{\partial Q_{b2}} = -2R_2 \frac{(Q_2 - Q_{b2})}{{U_{TC}}^2}.10^{-3} + \Delta p_{b2} - P_2.\frac{\partial \Delta\eta_2\{Q_2 - Q_{b2}\}}{\partial Q_{b2}} \\ \frac{\partial \Delta P_3}{\partial Q_{b3}} = -2R_3 \frac{(Q_3 - Q_{b3})}{{U_{TC}}^2}.10^{-3} + \Delta p_{b3} - P_3.\frac{\partial \Delta\eta_3\{Q_3 - Q_{b3}\}}{\partial Q_{b3}} \\ \frac{\partial \Delta P_{Trt}}{\partial Q_{bTrt}} = -2R_{td} \frac{(Q_\Sigma - Q_{\Sigma b} - Q_{btr})}{{U_{ht1}}^2}.10^{-3} + \Delta p_{bTrt} \end{cases} \quad (16)$$

Take the first derivative from Equation (3) $\frac{\partial \Delta\eta\{Q_{tt} - Q_b\}}{\partial Q_b}$; the following equation system can be achieved.

$$\begin{cases} \frac{\partial \Delta\eta_1\{Q_1 - Q_{b1}\}}{\partial Q_{b1}} = \left(2K_1.\Delta U_{Dc1}.\frac{\partial \Delta U_{Dc1}}{\partial Q_{b1}} + K_2.\frac{\partial \Delta U_{Dc1}}{\partial Q_{b1}}\right) \times 10^{-2} \\ \frac{\partial \Delta\eta_2\{Q_2 - Q_{b2}\}}{\partial Q_{b2}} = \left(2K_1.\Delta U_{Dc2}.\frac{\partial \Delta U_{Dc2}}{\partial Q_{b2}} + K_2.\frac{\partial \Delta U_{Dc2}}{\partial \Delta Q_{b2}}\right) \times 10^{-2} \\ \frac{\partial \Delta\eta_3\{Q_3 - Q_{b3}\}}{\partial Q_{b3}} = \left(2K_1.\Delta U_{Dc3}.\frac{\partial \Delta U_{Dc3}}{\partial Q_{b3}} + K_2.\frac{\partial \Delta U_{Dc3}}{\partial Q_{b3}}\right) \times 10^{-2} \end{cases} \quad (17)$$

Where $\Delta U_{Dc1}, \Delta U_{Dc2}$ and ΔU_{Dc3} denote the voltage drops in percentages of induction motor 1, induction motor two and induction motor 3, respectively.

According to Equation (4), it is necessary to deduce the following equation system:

$$\begin{cases} \frac{\partial \Delta U_{Dc1}}{\partial Q_{b1}} = -\frac{10^2}{U_{dm}}.\frac{\partial \Delta U_1}{\partial Q_{b1}} \\ \frac{\partial \Delta U_{Dc2}}{\partial Q_{b2}} = -\frac{10^2}{U_{dm}}.\frac{\partial \Delta U_2}{\partial Q_{b2}} \\ \frac{\partial \Delta U_{Dc3}}{\partial Q_{b3}} = -\frac{10^2}{U_{dm}}.\frac{\partial \Delta U_3}{\partial Q_{b3}} \end{cases} \quad (18)$$

Where $\Delta U_1, \Delta U_2$ and ΔU_3 are voltage drops from busbars induction motor 1, induction motor two and induction motor 3, respectively. Meanwhile, U_{dm} denotes the rated voltage of induction motors.

The three voltage drops mentioned above can be calculated as follows:

$$\begin{cases} \Delta U_1 = \frac{P_1.R_1 + (Q_1 - Q_{b1})X_1}{U_{TC}} \\ \Delta U_2 = \frac{P_2.R_2 + (Q_2 - Q_{b2})X_2}{U_{TC}} \\ \Delta U_3 = \frac{P_3.R_3 + (Q_3 - Q_{b3})X_3}{U_{TC}} \end{cases} \quad (19)$$

Where R_1, R_2 and R_3 are resistive components of the cables connecting the busbar to the induction motors. Similarly, X_1, X_2 and X_3 are the corresponding reactance components. U_{TC} denotes the voltage of the busbar.

According to Equations (16), (17), (18) and (19), it is significant to calculate compensations to minimize loss ΔP. These Equations are expressed below:

$$\begin{cases} Q_{b1} = Q_1 + \frac{2.10^2.K_1.P_1.X_1.(I) + K_2.P_1.X_1.U_{dm}.U_{TC} - (\Delta p_{b1} - \Delta p_{b\_Trt})(U_{dm}.U_{TC})^2}{2R_1.10^{-3}.U_{dm}^2 - 2.10^2.K_1.P_1.{X_1}^2} \\ Q_{b2} = Q_2 + \frac{2.10^2.K_1.P_2.X_2.(II) + K_2.P_2.X_2.U_{dm}.U_{TC} - (\Delta p_{b2} - \Delta p_{b\_Trt})(U_{dm}.U_{TC})^2}{2R_2.10^{-3}.U_{dm}^2 - 2.10^2.K_1.P_2.{X_2}^2} \\ Q_{b3} = Q_3 + \frac{2.10^2.K_1.P_3.X_3.(III) + K_2.P_3.X_3.U_{dm}.U_{TC} - (\Delta p_{b3} - \Delta p_{b\_Trt})(U_{dm}.U_{TC})^2}{2R_3.10^{-3}.U_{dm}^2 - 2.10^2.K_3.P_3.{X_3}^2} \\ Q_\Sigma - Q_{b\Sigma} - Q_{bTrt} = \frac{\Delta p_{bTrt}.U_{ht1}^2}{2R_{td}.10^{-3}} \end{cases} \quad (20)$$

$$\text{Where, }\begin{cases}(I) = [(U_{TC}.10^3 - U_{dm})U_{TC} - P_1.R_1] \\ (II) = [(U_{TC}.10^3 - U_{dm})U_{TC} - P_2.R_2] \\ (III) = [(U_{TC}.10^3 - U_{dm})U_{TC} - P_3.R_3]\end{cases} \quad (21)$$

Taking the second order of derivative ΔP_Σ, the result is positive. Therefore, the total power losses regarding three induction motors calculated in Equation (9) will obtain the minimal value when applying three decentralized compensators and a centralized one.

2.3. Simulation and Practical Application

In order to demonstrate the applicability of the proposed control method, a typical power system with three large-capacity induction motors is selected. The paper's Appendices provide simulation parameters for such a case study. It is noted that a NEMA curve is also chosen for approximating factors given in Equation (3). The corresponding curve is plotted in Figure 6.

A voltage deviation factor is considered to evaluate the proposed compensation method's performance. This factor is assumed to change in a normal range (0.9 to 1.1, corresponding to 90% to 110% of the rated voltage).

Calculated parameters, especially reactive power compensation values for three induction motors, and the total active power losses are presented in Table 1 and Table 2. It is clear from these two tables with calculated reactive power compensations that the active power losses at each load and in the whole system are significantly reduced from 3.5 to 21.3%, confirming the feasibility of the proposed method. Regarding the active power compensations, Figure 7 and Figure 8 illustrate these values in response to the change of voltage factor k. Figure 8 describes power compensations for a time-by-time random and continuous voltage change factor between a range of [0.9; 1.1]. Despite such a random variation, the system embedding the proposed compensators can optimize reactive power compensations and minimize active power losses.

To verify the practical application of the proposed method, accurate and larger loads are employed in a metropolitan building in Hanoi – the capital of Vietnam. They contain three huge loads: the 2-M1 Viettel building, a mechanical factory and the experiment building M1 Viettel. Practical results applying the proposed approach are plotted in Figure 9 to Figure 11. These Figures show that practical power losses and voltage drops are considerably reduced, leading to the possible applicability of the proposed compensation scheme.

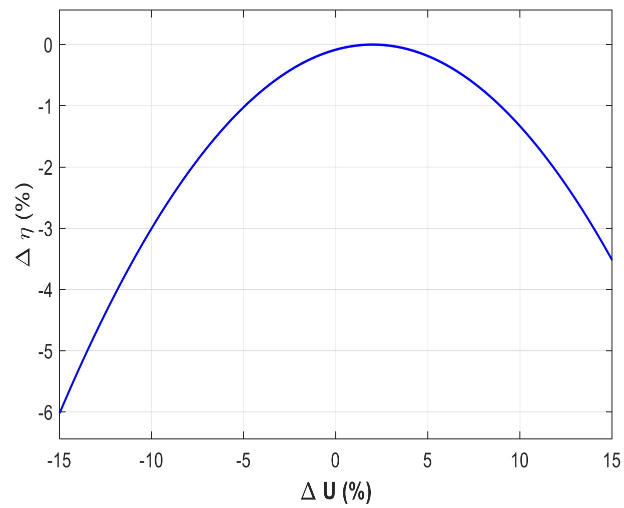

Fig. 6 The NEMA curve under study

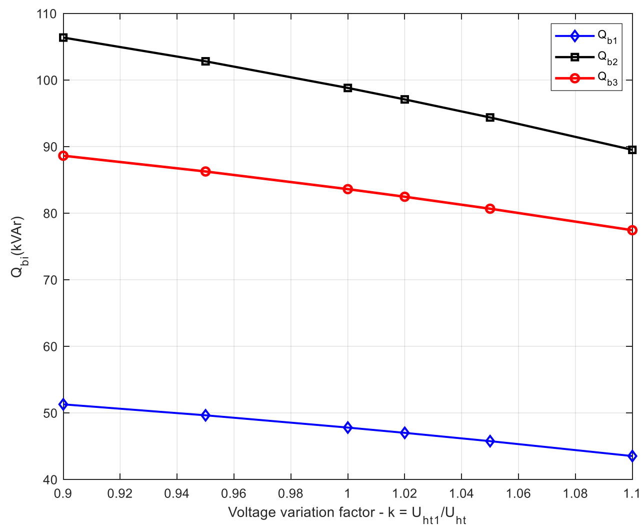

Fig. 7 An illustration of reactive power compensations for three induction motors concerning different voltage deviation factors

Table 1. Results of compensation for different voltage deviation factors (0.9 – 1.0)

Parameters	Power losses								
	U = 0.9*Udm			U = 0.95*Udm			U = 1.0*Udm		
	Before compensa-tion	After compensa-tion	Decrease (%)	Before compensa-tion	After compensa-tion	Decrease (%)	Before compensa-tion	After compensa-tion	Decrease (%)
Qb1 (kVAr)		51.3			49.6			47.8	
Qb2(kVAr)		106.4			102.8			98.8	
Qb3(kVAr)		88.6			86.3			83.6	
ΔP1(kW)	17349.1	15284.0	11.9	13910.5	12348.7	11.2	11605.7	10481.5	9.7
ΔP2(kW)	36299.5	29640.7	18.3	28931.2	23645.1	18.3	23658.4	19555.2	17.3
ΔP3(kW)	39893.9	32892.4	17.6	32515.9	26301.5	19.1	26523.9	21546.5	18.8
ΔP(kW)	93542.4	77817.1	16.8	75357.6	62295.4	17.3	61788.0	51583.2	16.5

Table 2. Results of compensation for different voltage deviation factors (1.02 – 1.1)

Parameters	Power losses								
	U = 1.02*Udm			U = 1.05*Udm			U = 1.1*Udm		
	Before compensa-tion	After compensa-tion	Decrease (%)	Before compensa-tion	After compensa-tion	Decrease (%)	Before compensa-tion	After compensa-tion	Decrease (%)
Qb1(kVAr)		47.0			45.8			43.5	
Qb2(kVAr)		97.1			94.4			89.5	
Qb3(kVAr)		82.5			80.7			77.4	
ΔP1(kW)	10993.6	10028.6	8.8	10401.8	9660.6	7.1	10273.0	9868.5	3.9
ΔP2(kW)	22115.0	18439.2	16.6	20390.4	17312.4	15.1	19055.8	16870.2	11.5
ΔP3(kW)	24671.8	20140.5	18.4	22457.7	18549.6	17.4	20227.7	17249.2	14.7
ΔP(kW)	57780.5	48608.4	15.9	53249.9	45522.5	14.5	49556.5	43988.0	11.2

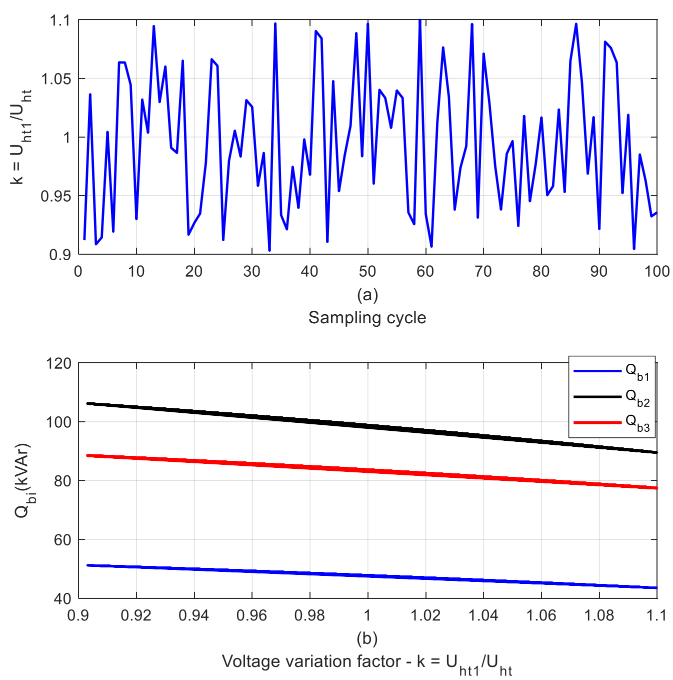

Fig. 8 Reactive power compensations for three induction motors concerning random voltage deviation factors between 0.9 and 1.1

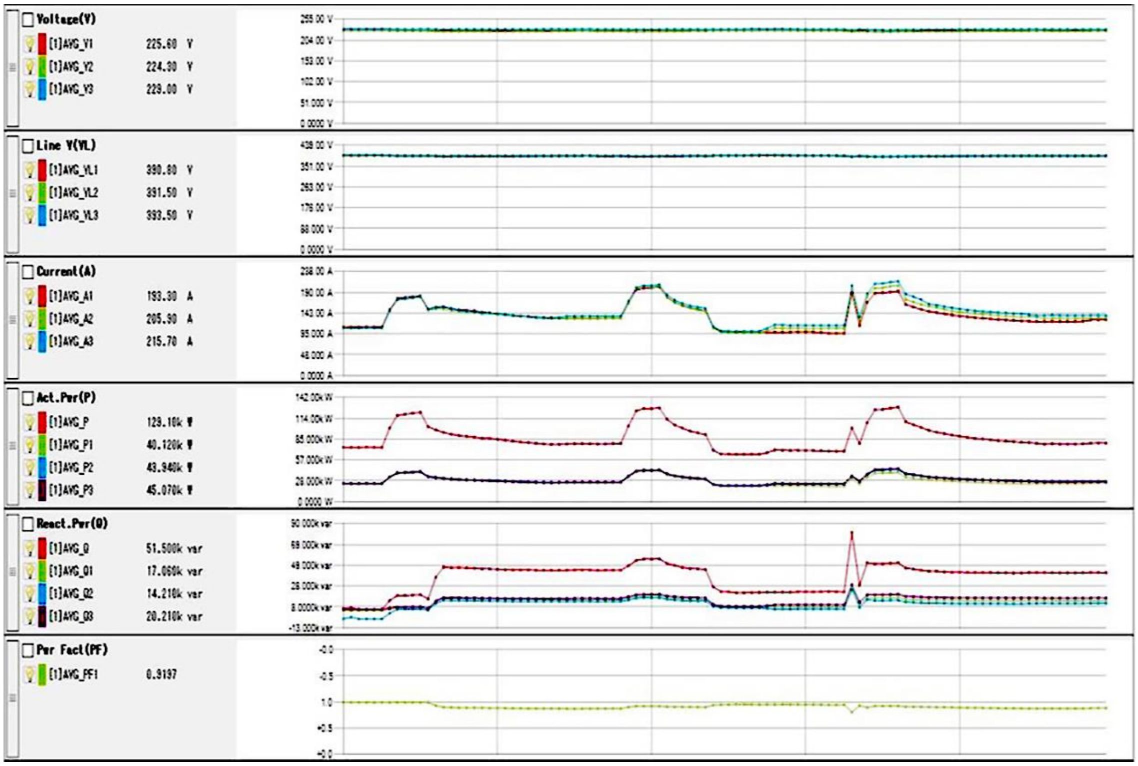

(a)

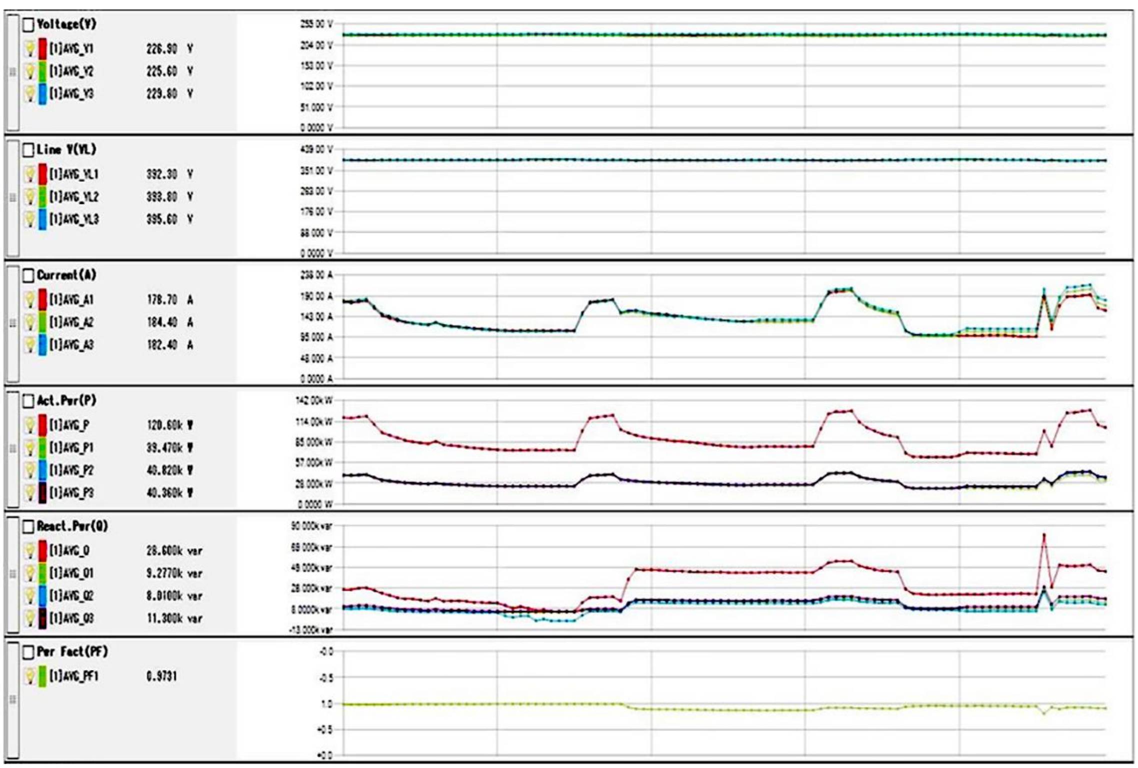

(b)

Fig. 9 Practical evaluation of the proposed compensation strategy at the 2-M1 Viettel building (in Hanoi – Vietnam) (a) Before compensation (b) After compensation

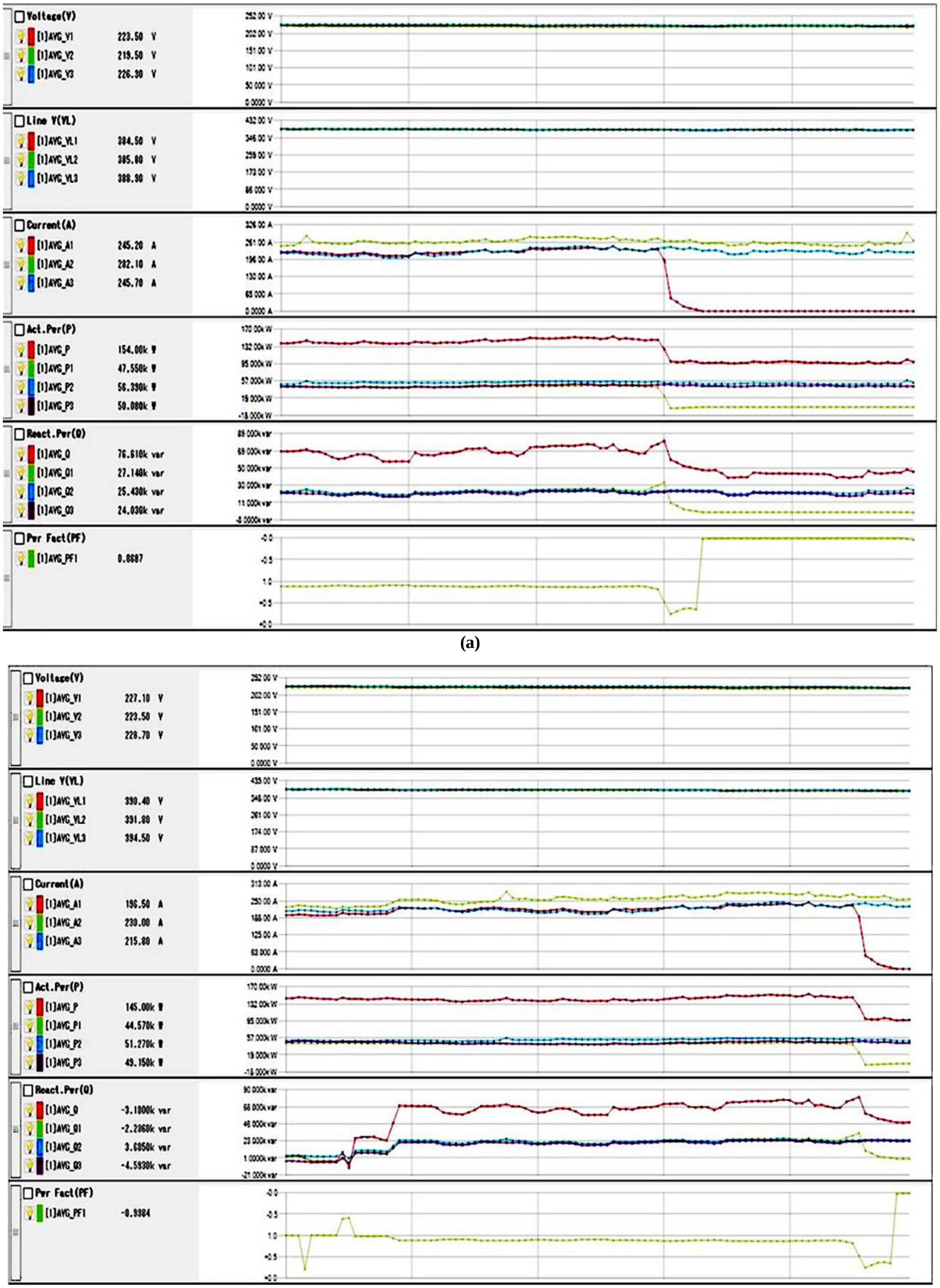

(a)

(b)

Fig. 10 Practical evaluation of the proposed compensation strategy at the mechanical factory (in Hanoi – Vietnam) (a) Before compensation (b) After compensation

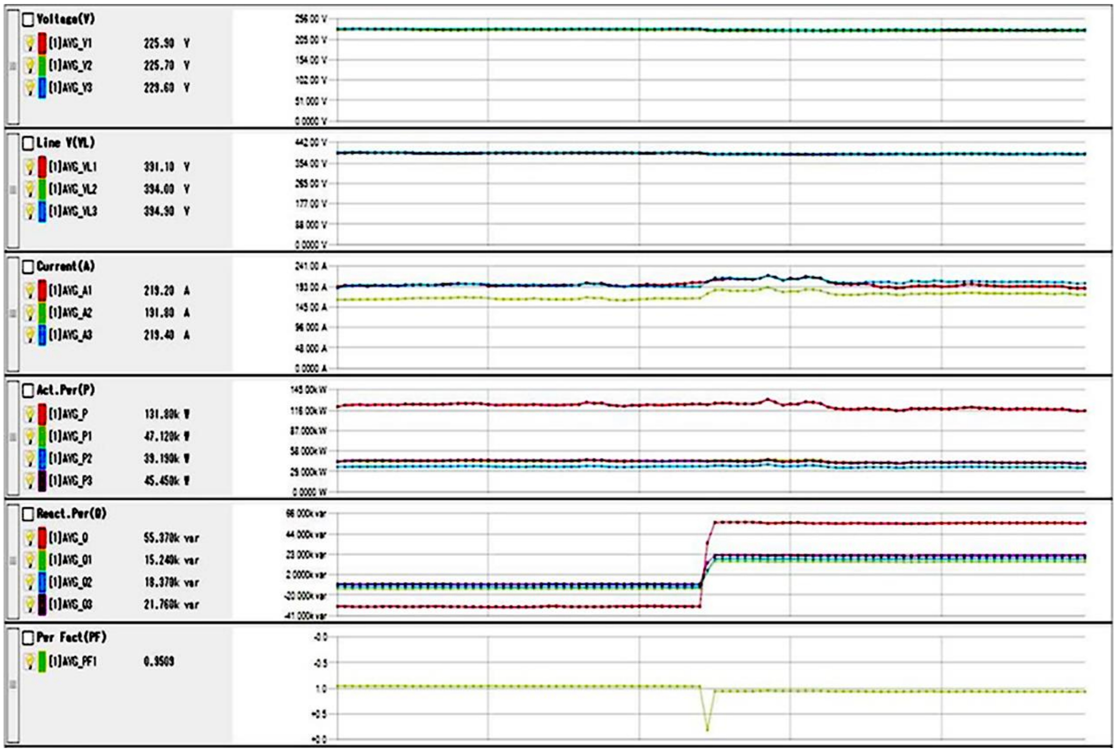

(a)

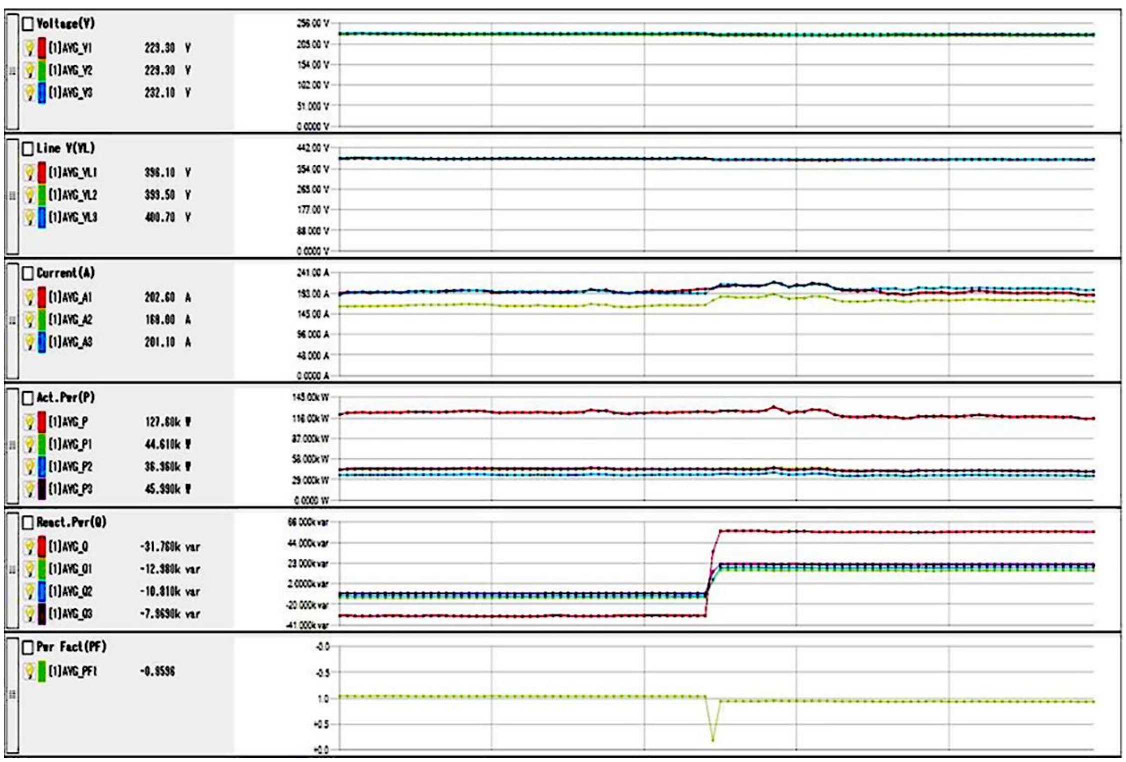

(b)

Fig. 11 Practical evaluation of the proposed compensation strategy at the experiment building M1-Viettel (in Hanoi – Vietnam) (a) Before compensation (b) After compensation

3. Conclusion and Future Work

This paper has analyzed a significant interaction between power quality and efficiency of large-capacity induction motors in an electric power grid. Then, a new control scheme to calculate fast reactive power compensations for the asynchronous AC motors and, thereby, minimize the active power of the whole system has been successfully designed in this study. Despite a more complicated operation mechanism, the proposed method obtained much better performance in compassion than its regular centralized counterparts. The studied compensation strategy applying the decentralized compensators assists to obtain better voltage regulation by reducing the voltage drops at each load. This meaningful feature ensures efficient operation of electric equipment, energy saving and enhancing the lifetime of the devices.

Future work will apply the proposed compensating methodology for a more extensive system containing many inductions motors and other vital loads.

Appendix

Table 3. System parameters under study

Parameters	Value	Unit
Uht1=k.Udm		kV
Udm	400	V
Rtd	0.0022	Ω
Xtd	0.00892	Ω
Psum	372	kW
Q	8.79958	kVAr
DeltaU	0.002	kV
Utc		kV
Δp_{bTrt}	$0.2*10^{-3}$	kW/ kVAr
K1 (NEMA factor)	- 0.02083	n/a
K2 (NEMA factor)	0.08333	n/a
C (NEMA factor)	- 0.0833	n/a

Table 4. Parameters of induction motor 1 and Cable 1

Induction motor 1 and cable 1	Value	Unit
R1	0.0525	Ω
X1	0.0109	Ω
P1	90	kW
Q1	46.11	kVAr
cosφ	0.85	
Efficiency	93	%
Δp_{b1}	$0.5*10^{-3}$	kW/kVAr

Table 5. Parameters of motor 2 and cable 2

Induction motor 2 and cable 2	Value	Unit
R2	0.0514	Ω
X2	0.0142	Ω
P2	150	kW
Q2	92.96	kVAr
cosφ	0.85	
Efficiency	93	%
Δp_{b2}	$0.5*10^{-3}$	kW/kVAr

Table 6. Parameters of motor 3 and cable 3

Induction motor 3 and cable 3	Value	Unit
R3	0.0875	Ω
X3	0.0182	Ω
P3	132	kW
Q3	78.32	kVAr
cosφ	0.86	
Efficiency	93	%
Δp_{b3}	$0.5*10^{-3}$	kW/kVAr

References

[1] Bhim Singh et al., "Reactive Power Compensation and Load Balancing in Electric Power Distribution Systems," *International Journal of Electrical Power & Energy Systems*, vol. 20, no. 6, pp. 375-381, 1998. [CrossRef][Google Scholar][Publisher Link]

[2] Danilo I. Brandao et al., "Centralized Control of Distributed Single-Phase Inverters Arbitrarily Connected to Three-Phase Four-Wire Microgrids," *IEEE Transactions on Smart Grid*, vol. 8, no. 1, pp. 437-446, 2017. [CrossRef][Google Scholar][Publisher Link]

[3] Daniel E. Olivares et al., "Trends in Microgrid Control," *IEEE Transactions on Smart Grid*, vol. 5, no. 4, pp. 1905–1919, 2014. [CrossRef][Google Scholar][Publisher Link]

[4] A. Khodaei, "Provisional Microgrids," *IEEE Transactions on Smart Grid*, vol. 6, no. 3, pp. 1107–1115, 2015. [CrossRef][Google Scholar][Publisher Link]

[5] T. Devaraju, V. C. Veera Reddy, and M. Vijaya Kumar, "Role of Custom Power Devices in Power Quality Enhancement: A Review," *International Journal of Engineering Science and Technology*, vol. 2, no. 8, pp. 3628–3634, 2010. [Google Scholar]

[6] Omkar Pawar, P. Marshall Arockia Dass, and A. Peer Fathima, "Power Quality Improvement using Compensating Type Custom Power Devices: A Review," *National Conference on Science, Engineering and Technology*, vol. 4, no. 6, pp. 155–158, 2016. [Publisher Link]

[7] Sumit Mazumder Ami, "Power Quality Improvements in Low Voltage Distribution Networks Containing Distributed Energy Resources," Queensland University of Technology, 2015. [Google Scholar][Publisher Link]

[8] Mohammed Osman, and Bahr Eldin Suliman, "*Power Quality Improvement of A Distribution System Based on New Custom Power Devices*," Universiti Teknologi Petronas, Sudan, 2014. [Google Scholar][Publisher Link]

[9] Enrique Ciro Quispe et al., "Unbalanced Voltages Impacts on the Energy Performance of Induction Motors," *International Journal of Electrical and Computer Engineering*, vol. 8, no. 3, pp. 1412-1422, 2018. [CrossRef][Google Scholar][Publisher Link]

[10] P. O. Oluseyi et al., "Assessment of the Influence of Voltage Unbalance on Three-Phase Operation of Power System," *Nigerian Journal of Technology*, vol. 40, no. 5, pp. 901–912, 2021. [CrossRef][Google Scholar][Publisher Link]

[11] Ching Yin Lee, "Effects of Unbalanced Voltage on the Operation Performance of A Three-Phase Induction Motor," *IEEE Transactions on Energy Conversion*, vol. 14, no. 2, pp. 202-208, 1999. [CrossRef][Google Scholar][Publisher Link]

[12] Pragasen Pillay, and Marubini Manyage, "Loss of Life in Induction Machines Operating with Unbalanced Supplies," *IEEE Transactions on Energy Conversion*, vol. 21, no. 4, pp. 813-822, 2006. [CrossRef][Google Scholar][Publisher Link]

[13] Miloje Kostić, "Equivalent Circuit and Induction Motor Parameters for Harmonics Studies in Power Networks," *Eletrotehniski Vetstnik*, vol. 79, no. 3, pp. 135–140, 2012. [Google Scholar][Publisher Link]

[14] Oladokun E. Faduyile, "Effect of Harmonics on the Efficiency of a Three Phase Energy Efficient and Standard Motors," *Masters Theses, University of Tennessee at Chattanooga*, Chattanooga (Tenn.), 2009. [Google Scholar][Publisher Link]

[15] A. H. Bonnett, "The Impact that Voltage and Frequency Variations have on AC Induction Motor Performance and Life in Accordance with NEMA MG-1 standards," *Conference Record of 1999 Annual Pulp and Paper Industry Technical Conference (Cat. No.99CH36338)*, Seattle, WA, USA, pp. 16-26, 1999. [CrossRef][Google Scholar][Publisher Link]

[16] Rui Esteves Araujo, "Induction Motors - Modelling and Control," InTech, 2012. [CrossRef] [Google Scholar] [Publisher Link]

[17] A. H. Bonnett, "An Overview of How AC Induction Motor Performance has been Affected by the October 24, 1997 Implementation of the Energy Policy Act of 1992," *Record of Conference Papers - IEEE Industry Applications Society 45th Annual Petroleum and Chemical Industry Conference (Cat. No.98CH36234)*, Indianapolis, IN, USA, 1998. [CrossRef] [Google Scholar] [Publisher Link]

[18] Miloje M. Kostic, and Branka B. Kostic, "Motor Voltage High Harmonics Influence to Efficient Energy Usage," *In Proceedings of the 15th WSEAS International Conference on Systems. Recent Researches in System Science*, WEAS Library, pp. 276-281, 2011. [Google Scholar] [Publisher Link]

[19] "NEMA Standards Publication MG 1-2006 Revision 1-2007 Motors and Generators," *National Electrical Manufacturers Association*, 2006.

[20] Paul Lemieux et al., "Transportable Gasifier for On-Farm Disposal of Animal Mortalities," *5th International Symposium on Managing Animal Mortality, Products*, pp. 1-10, 2015.[Google Scholar] [Publisher Link]

[21] Austin H. Bonnett, "The Impact that Voltage Variations have on AC Induction Motor Performance," *Conference Record of 1999 Annual Pulp and Paper Industry Technical Conference (Cat. No. 99CH36338)*, 1999.[Google Scholar] [Publisher Link]

[22] Nguyen Tien Dung, Dinh Ngoc Quang, and Bui Anh Tuan, "Voltage Quality Improvement for Induction Motor in Power System," *EPU Journal of Science and Technology for Energy*, vol. 22, no. 22, pp. 48-57, 2020.[Google Scholar]

[23] Nguyen Tien Dung, "Reactive Power Compensation in Distributed System using Centralized Control," *Journal of Military Science and Technology*, vol. 68, pp. 54–66, 2020. [Google Scholar] [Publisher Link]

[24] A. E. Kravčik, *Induction Machines*, Handbook, Moscow: Russian, pp. 504, 1982.

[25] "IEEE Recommended Practice for Monitoring Electric Power Quality," *IEEE Std 1159-2019 (Revision of IEEE Std 1159-2009)*, pp. 1-98, 2019. [CrossRef] [Google Scholar] [Publisher Link]

[26] IEC 61000-4-7 (1991), Electromagnetic Compatibility (EMC), Part 4: Limits, Section 7: General Guide on Harmonics and Equipment Connected Thereto, International Electrotechnical Committee, 1991. [Online] . Available: https://infostore.saiglobal.com/en-us/standards/iec-61000-4-7-1991-569842_saig_iec_iec_2993071https://infostore.saiglobal.com/en-us/standards/iec-61000-4-7-1991-569842_saig_iec_iec_2993071